Recent geodetic unrest at Santorini Caldera, Greece

Andrew V. Newman,[1] Stathis Stiros,[2] Lujia Feng,[1,3] Panos Psimoulis,[2,4] Fanis Moschas,[2] Vasso Saltogianni,[2] Yan Jiang,[5] Costas Papazachos,[6] Dimitris Panagiotopoulos,[6] Eleni Karagianni,[6] and Domenikos Vamvakaris[6]

Received 8 February 2012; revised 5 March 2012; accepted 6 March 2012; published 30 March 2012.

[1] After approximately 60 years of seismic quiescence within Santorini caldera, in January 2011 the volcano reawakened with a significant seismic swarm and rapidly expanding radial deformation. The deformation is imaged by a dense network of 19 survey and 5 continuous GPS stations, showing that as of 21 January 2012, the volcano has extended laterally from a point inside the northern segment of the caldera by about 140 mm and is expanding at 180 mm/yr. A series of spherical source models show the source is not migrating significantly, but remains about 4 km depth and has expanded by 14 million m^3 since inflation began. A distributed sill model is also tested, which shows a possible N-S elongation of the volumetric source. While observations of the current deformation sequence are unprecedented at Santorini, it is not certain that an eruption is imminent as other similar calderas have experienced comparable activity without eruption. **Citation:** Newman, A. V., et al. (2012), Recent geodetic unrest at Santorini Caldera, Greece, *Geophys. Res. Lett.*, *39*, L06309, doi:10.1029/2012GL051286.

1. Introduction

[2] Santorini Caldera, a mostly submerged volcanic complex in the southern Aegean, is part of a well developed, and very active system that began its volcanic history about 600 thousand years ago, due to subduction along the Hellenic arc [*Heiken and McCoy*, 1984; *Druitt et al.*, 1999]. About 1650 B.C. [*Friedrich et al.*, 2006], a series of massive Plinean eruptions expelled some 40 - 60 km^3 of volcanic material, collapsing the previous central island surface, forming the present caldera form, and causing a massive regional tsunami [*Heiken and McCoy*, 1984; *Sigurdsson et al.*, 2006]. Known as the Minoan eruption, the event is arguably the main cause of the demise of the seafaring Minoan civilization [*Hardy and Renfrew*, 1990; *Manning et al.*, 2006], of which a major port city of Akrotiri on Santorini was buried by more than 20 m of tephra. The five-island group, collectively called Santorini, exists today as an extremely popular tourist destination, with many of its villages situated on near-vertical encompassing cliffs created during the Minoan and previous caldera collapse events.

[3] Over the past 2000 years, the system has periodically been active with smaller pyroclastic and phreatic eruptions forming the central islets of Palea and Nea Kameni atop the submerged caldera floor. Since 1570 A.D., a series of 5 dacitic eruptions have occurred to form Nea Kameni through dome growth and blocky a'a flows, with the most recent activity ending in 1950 [*Heiken and McCoy*, 1984; *Pyle and Elliott*, 2006]. Since then, the caldera has remained quiet with only small and localized deformation [*Farmer et al.*, 2007; *Stiros et al.*, 2010]. Santorini has also remained practically aseismic with earthquakes occurring almost exclusively about 10 km outside the caldera to the northeast, at the submerged Columbo volcano [*Dimitriadis et al.*, 2009]. After 60 years of calm, early in 2011 the caldera appeared to reawaken with rapidly increasing earthquake activity and ground deformation (Figure 1).

2. The 2011 Unrest

2.1. Seismicity

[4] On 9 January 2011 an anomalous sequence of earthquakes began inside the caldera, the first substantial activity observed within the caldera with modern seismographic networks [e.g., *Dimitriadis et al.*, 2010], and possibly the most significant since the last eruptive sequence ending in 1950. Seismicity is recorded by a growing local network of up to 10 seismometers operated by the Aristotle University of Thessaloniki and the Institute for the Study and Monitoring of Santorini Volcano (ISMOSAV). Between 9 January 2011 and 21 January 2012 earthquakes have remained below local magnitude $M_L \leq 3.2$, outlining a nearly vertical fault directly beneath the Kameni islets. Earthquakes occur primarily between 1 and 6 km depth and extend laterally toward the main village of Thira (area surrounding station NOMI in Figure 1). This fault, possibly a ring fracture created during the Minoan eruption, is the site of the prior intra-caldera eruptions over the past millennium, forming the Kameni islets. At the time of this manuscript submission (January 2012), frequent intra-caldera seismicity is ongoing with seismicity frequently in excess of 10 events per day with $M_L \geq 1.0$, the magnitude of completeness through 2011 (Figure 1).

2.2. GPS

[5] In 2006, research teams at Georgia Tech and the University of Patras established a GPS network, consisting of 19 survey and 3 continuous GPS (cGPS) stations. Data

[1]School of Earth and Atmospheric Sciences, Georgia institute of Technology, Atlanta, Georgia, USA.
[2]Department of Civil Engineering, University of Patras, Patras, Greece.
[3]Now at Earth Observatory of Singapore, Nanyang Technological University, Singapore.
[4]Now at Institute of Geodesy and Photogrammetry, Zurich, Switzerland.
[5]Rosenstiel School of Marine and Atmospheric Sciences, University of Miami, Miami, Florida, USA.
[6]Geophysical Laboratory, Aristotle University of Thessaloniki, Thessaloniki, Greece.

0094-8276/12/2012GL051286

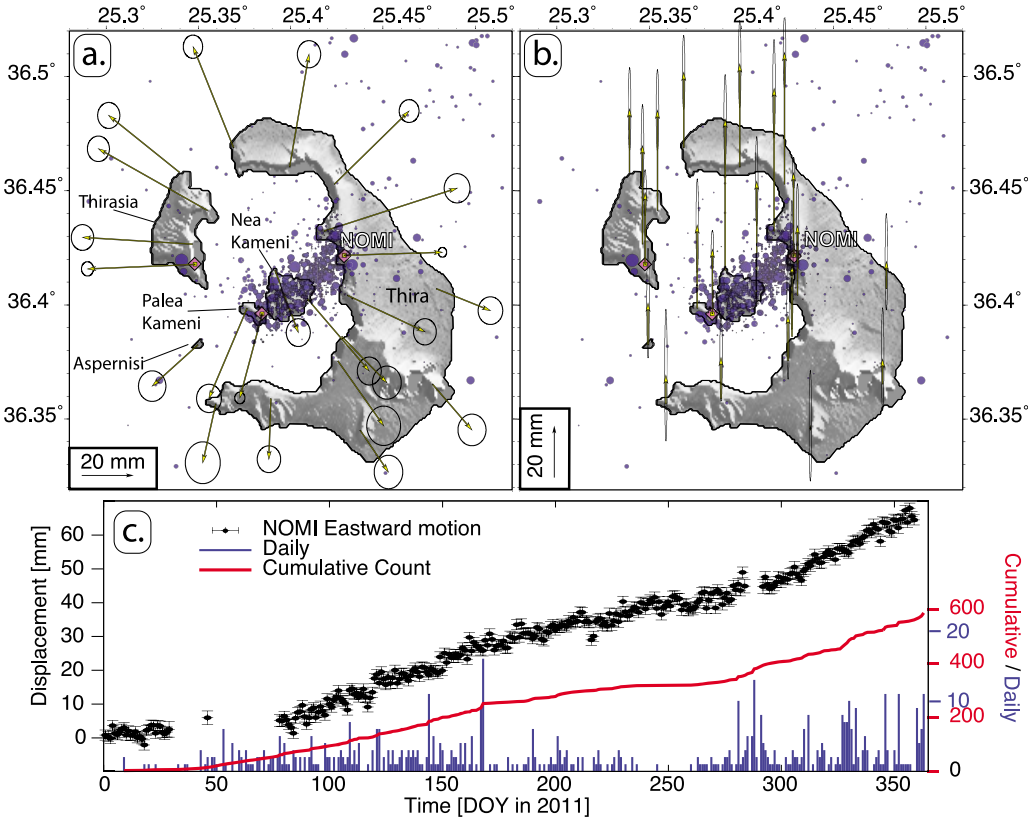

Figure 1. Map view of the (a) horizontal and (b) vertical displacement field with scaled seismicity (local magnitude $M_L \leq 3.2$; blue) in 2011. 19 campaign and 3 continuous GPS (magenta diamonds) show near radial displacements between their last observation in 2010 and late-August 2011. (c) The temporal evolution of seismicity ($M_L \geq 1.0$, the observed level of completeness) and GPS as represented by the eastward component of station NOMI are also shown. The cumulative number of earthquakes mimics the inflation shown.

from the cGPS, and surveys in 2006, 2008, and 2010 showed virtually no motion across the caldera (Figure S1 in the auxiliary material) resulting in relatively slow, but poorly constrained convergence through 2010 across the 7.2 km NOMI-KERA baseline, yielding a strain rate $\dot{\varepsilon}$ of less than -10^{-6} yr^{-1} (strain is defined as positive in extension).[1] Details of GPS processing are explained in Text S1.

[6] However, beginning in early 2011, significant local movements became apparent, and two surveys were conducted to establish the deformation across the network, and improve cGPS infrastructure. The first survey was conducted in June 2011 (hereafter 2011-I) with limited funding that only allowed for only occupation of 11 stations, and temporarily repair of cGPS sites PKMN and KERA. GPS between 2010 and 2011-I showed that most stations extended outward from the northern caldera between 5 and 32 mm (Figure S2). Only NOMI captured the onset of deformation around the beginning of 2011, but it is reasonable to expect deformation at all sites started about the same time (Figure 2). By 2011-I, approximately 45 mm of extension was observed between NOMI and KERA corresponding to an extensional $\dot{\varepsilon} = 13.7 \times 10^{-6}$ yr^{-1}.

[7] From these results, funds were acquired from the National Science Foundation (NSF) for a rapid deployment to perform a complete GPS survey, improve the infrastructure on the existing cGPS stations, and establish 2 new cGPS sites in the northern section of the caldera in late-August/early-September 2011 (hereafter 2011-II). Data from all cGPS are collected through automated telemetry, and for hazards assessment are processed at the University of Miami using GIPSY for low-latency and final daily solutions (Figure 2). After the 2011-II survey, the radial expansion first observed in June was more constrained with both additional sites and longer observations (Figures 1 and 3). Lateral displacements increased to between 19 and 54 mm, with the NOMI-KERA baseline showing 79 mm of extension, corresponding to $\dot{\varepsilon} = 16.7 \times 10^{-5}$ yr^{-1}. Though fluctuations in the rate of deformation are apparent from cGPS, the orientation of the displacement vectors is similar, suggesting the source is not migrating significantly. The 5 cGPS stations in operation between 2011-II and 21 January 2012 show a similar pattern, but increase in rate to 180 mm/yr corresponding to $\dot{\varepsilon} = 2.5 \times 10^{-5}$ yr^{-1}, with the total expansion across the NOMI-KERA baseline at approximately 140 mm.

3. Models

[8] For volcanic bodies, deformation is often described by simple volumetric changes of spherical sources [*Mogi*, 1958; *McTigue*, 1987], ellipsoidal sources [*Yang et al.*, 1988], horizontal penny-shaped cracks [*Fialko et al.*, 2001], or by

[1]Auxiliary materials are available in the HTML. doi:10.1029/2012GL051286.

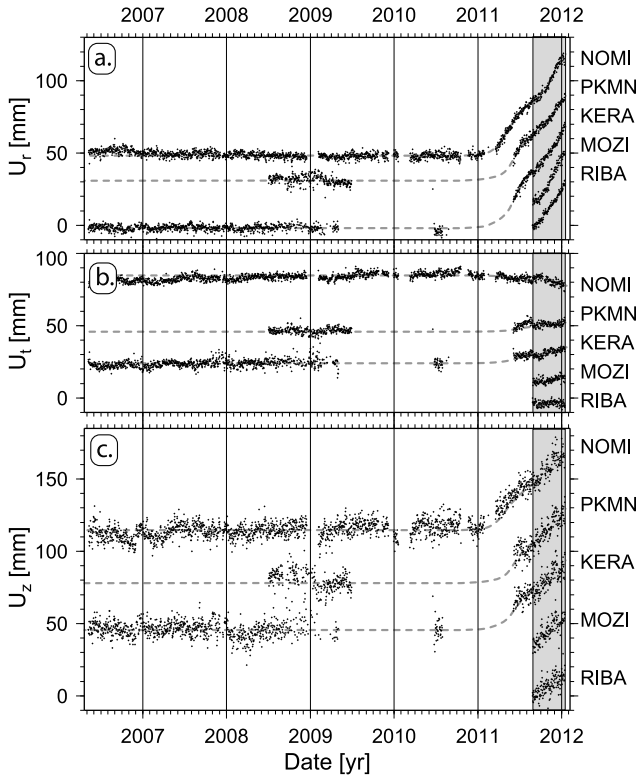

Figure 2. Time series showing the relative (a) radial (U_r), (b) transverse (U_t) and (c) vertical (U_t) components of 5 continuous GPS stations used in this study. The radial and transverse horizontal components are rotated relative to the best-fitting source shown in Figure 3. For all time series, the average pre-2011 motion of Santorini is removed (East, North = 7.06, −15.78 mm/yr). Stations RIBA and MOZI were both installed late August 2011. The vertical gray bar highlights the period shown in Figure 4, after 2 new continuous GPS are operational. Dashed lines are solely to connect the discontinuous time series and are not meant for any other interpretation.

opening or slipping rectangular dislocations [*Okada*, 1985]. Each have their advantage for particular volcanic provinces, and often a number can be explored. Because the ongoing deformation at the time of this writing appears to be well described by a largely axi-symmetric source, as evidenced by the lack of substantial tangential motion in Figure 2, we focus on the *Mogi* [1958] spherical source model due to its simplicity, but also explore a distributed sill model to evaluate a potentially more complex source geometry.

[9] We identified the best fit solutions between the three-dimensional (3D) GPS data and model solutions for the volumetric change ΔV and 3D position of an expanding spherical source following *McTigue*'s [1987] formulism of *Mogi* [1958] (Figure 3). Such a model requires only the assumption that a small spherical source is radially expanding in a homogeneous elastic Poisson half-space. Following an iterative grid search method used by *Feng and Newman* [2009], we use an apriori estimate of ΔV and depth z to initially constrain a preferred horizontal position. Using this position a new best fit z and ΔV is determined, which are again used as input for a repeated grid search to refine the location and ΔV for improved final solutions.

[10] Results from the limited data from the 2011-I survey are comparable in position but smaller in magnitude to the results from the 2011-II survey (Figures 2 and 3). The two models show practically the same source location centered in the northern caldera approximately 1–2 km north of Nea Kameni and about 4 km depth (Table 1). The cumulative volume change increased from approximately 4 to 7 million m^3 between 2011-I and 2011-II surveys.

[11] Using the 5 cGPS between the 2011-II survey (when 2 new cGPS were installed) and 21 Jan. 2012, we again find a similar lateral, but modestly deeper best fit source (z = 4.8 km). The observed changes are much less than the uncertainties in the solutions, and hence we do not infer that the source has migrated appreciably. For this period the rate of volumetric growth was 22.1 million m^3/yr at the best fit depth, corresponding to an additional ΔV of 9.2 million m^3,

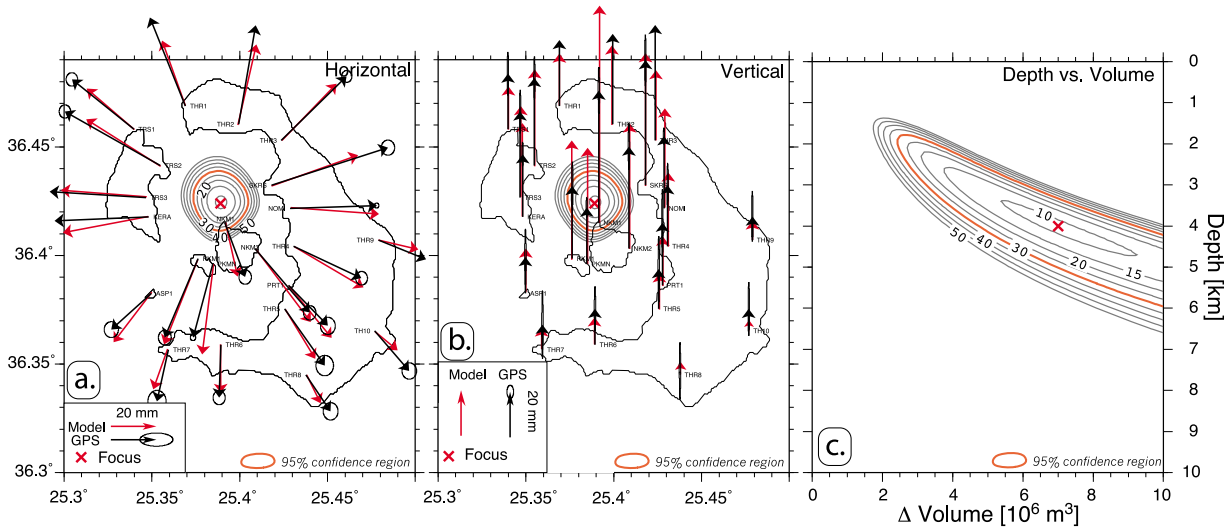

Figure 3. (a) Horizontal and (b) vertical model predictions and solution for spherical source that well describe the observed deformation field. Also shown is (c) the depth vs. volume trade-off. Reduced chi-square error contours are shown with their 95% confidence interval (red).

Table 1. Model Parameters

Date Range	Latitude (deg)	Longitude (deg)	Z (km)	ΔV ($\times 10^6$ m^3)	$\Delta \dot{V}$ ($\times 10^6$ m^3 yr^{-1})	rms (cm)
2010 to 2011-I	36.426	25.390	3.9	4.1	9.5	1.13
2010 to 2011-II	36.424	25.389	4.0	7.0	10.6	0.84
2010 to 2011-II (Sill)[a]	36.43	25.39	4.0	9.2	14.2	1.50
2011-II to 21 Jan. 2012[b]	36.423	25.389	4.0	9.0	17.4	2.71
2010 to 21 Jan. 2012 (compiled)	36.424	25.389	4.0	14.1	13.4	-

[a]Sill solution used a fixed depth; horizontal position is the SW corner of 0.01° × 0.01° element with maximum opening (82.1 cm).
[b]Preferred solution at 4.0 km depth is shown rather than the best-fit solution at 4.8 km.

for the 5-month period (Figures 4 and S3). Because determinations of ΔV are sensitive to z, which is poorly constrained due to the reduced quality of the vertical GPS and sub-optimal distal distribution of the cGPS from the source, we prefer a solution holding z fixed at 4 km, similar to earlier results, yielding 7.1 million m^3 of additional volumetric growth.

[12] As an alternative model, we follow *Okada* [1985] to develop a distributed sill model using 144 − 0.01° × 0.01° km patches, again at 4 km depth, and invert the model to fit the 2010 to 2011-II surveys. We apply a Laplacian smoothing constraint to control the interdependence of model nodes, and avoid an overly rough model solution [*Harris and Segall*, 1987]. The results from this model agree with the previous models, with the majority of deformation coming from a source in the center of the northern section of the caldera (Figure S4). The solutions increase the rms misfit by a factor of two over the spherical source model using the same data (Table 1). Likewise, the solutions are highly non-unique and dependent on the smoothing-level chosen, thus we consider this model to be ill-suited to constrain the source. The results are, however useful as they illuminate a possible elongated source in the north-south direction.

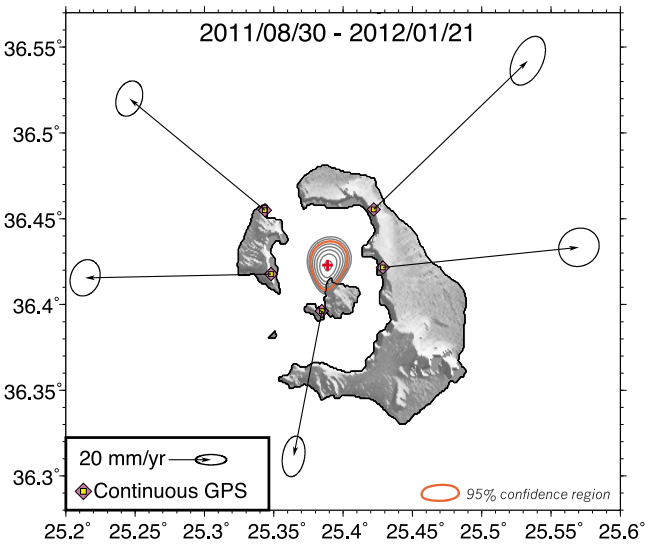

Figure 4. Map view of the most recent expansion between 1 September 2011 and 21 January 2012, the period after the last campaign but including two northernmost continuous GPS sites. While the best-fit source remains similar in location to the earlier period of unrest through September 2011 (Figures 1 and 3), the rate of volumetric growth is increased. Using the preferred depth of 4 km, $\Delta V = 17.4 \times 10^6$ m^3/yr (see Figure S2). Reduced chi-square error contours are shown with their 95% confidence interval (red).

4. Interpretation

[13] As seen in other active silicic calderas, including Long Valley [*Newman et al.*, 2006; *Feng and Newman*, 2009] and Yellowstone [*Chang et al.*, 2007], and the recently erupting Eyjafjallajökull stratovolcano [*Sigmundsson et al.*, 2010], the temporal occurrence of seismicity mimics observed deformation (Figure 1). Each change in the cumulative seismicity marks a similar change in the rate of deformation. Increases in seismic activity signal increasing deformation, while a relative cessation in earthquakes in June marks a point where deformation begins to slow. Though the concurrence of seismicity and ground deformation suggests the same source for geophysical unrest at Santorini, the spatial distribution of measurements from survey and cGPS reveal a near-radial volumetric expansion about 2 km north of the observed seismicity, at about 4 km depth. This pattern of deformation cannot be describe by deformation along a plane defining the seismicity, and thus it is more likely that the seismicity is responding to either regional stresses induced by the inflation source, or both the seismicity and deformation source are interconnected at depth and are concurrently excited by deeper pressure changes.

[14] Combining the modeled source growth from the 2010 to 2011-II, and the 2011-II to Jan. 2012 models results in ΔV = 14.1 million m^3 for a source at 4 km depth. This inflation is only about 0.03% the estimated eruptive volume of the 1650 B.C. eruption [*Sigurdsson et al.*, 2006], and thus the material added between 2011 and early 2012 alone is not sufficient to cause a repeat of a Minoan-style eruption. Instead, it is possible that this event will either result in a much smaller eruption, or that it will contribute to long-term dome growth. In other caldera systems, most notably the Valles Caldera in New Mexico, the development of a nearly 1 km high resurgent dome appeared to have completed within about 50 ky after formation [*Phillips*, 2004]. It is reasonable to suggest that such dome growth is episodically occurring at Santorini, less than 4 ky after its last caldera forming event.

5. Conclusion

[15] The intra-caldera seismicity and ground deformation rates observed between 2011 and early 2012 are unprecedented and likely the largest such activity since the 1950 eruption. Inflation of a likely magmatic source has caused 5 to 9 cm or radial expansion observed at 24 GPS sites across the caldera. Spherical source models prefer a source about

4 km depth in the northern half of the caldera, with a cumulative expansion of 14 million m^3 since inflation began. It is unclear how Santorini will proceed, and it is not certain that an eruption is imminent since similar deformation and seismicity patterns are observed at other silicic calderas, so far without eruption. However, should Santorini erupt, it is quite likely that it will be with smaller pyroclastic and/or phreatic activity, similar to that which has occurred over the past 440 years. Potentially more dangerous is the effect of volcanic ashfall and earthquake activity, which could damage houses, induce landslides along the steep caldera cliffs and cause local tsunamis that could be dangerous for the local boat traffic within the caldera.

[16] **Acknowledgments.** UNAVCO Facility support for data collection and archiving is possible with support from the NSF and NASA under NSF EAR-0735156. NSF support to AVN for Aug./Sept. campaign and network infrastructure under EAR-1153355. O. Karakas, Z. Lifton, C. Hopkins, G. Farmer, and J. Jackson helped in field surveys and continuous GPS installations.

[17] The Editor thanks Freysteinn Sigmundsson and an anonymous reviewer for their assistance in evaluating this paper.

References

Chang, W.-L., R. B. Smith, C. Wicks, J. M. Farrell, and C. M. Puskas (2007), Accelerated uplift and magmatic intrusion of the Yellowstone Caldera, 2004 to 2006, *Science*, *318*(5852), 952–956, doi:10.1126/science.1146842.

Dimitriadis, I., E. Karagianni, D. Panagiotopoulos, C. Papazachos, P. Hatzidimitriou, M. Bohnhoff, M. Rische, and T. Meier (2009), Seismicity and active tectonics at Coloumbo Reef (Aegean Sea, Greece): Monitoring an active volcano at Santorini Volcanic Center using a temporary seismic network, *Tectonophysics*, *465*, 136–149, doi:10.1016/j.tecto.2008.11.005.

Dimitriadis, I., C. Papazachos, D. Panagiotopoulos, P. Hatzidimitriou, M. Bohnhoff, M. Rische, and T. Meier (2010), P and S velocity structures of the Santorini–Coloumbo volcanic system (Aegean Sea, Greece) obtained by non-linear inversion of travel times and its tectonic implications, *J. Volcanol. Geotherm. Res.*, *195*(1), 13–30, doi:10.1016/j.jvolgeores.2010.05.013.

Druitt, T. H., L. Edwards, R. M. Mellors, D. M. Pyle, R. S. J. Sparks, M. Lanphere, M. Davies, and B. Barriero (1999), *Santorini Volcano*, *Geol. Soc. London Mem.*, *19*, 165 pp.

Farmer, G. T., A. V. Newman, P. Psimoulis, and S. Stiros (2007), Geodetic characterization of Santorini Caldera from continuous GPS measurements, *Eos Trans. AGU*, *88*(52), Jt. Assem. Suppl., Abstract G43B-1195.

Feng, L., and A. V. Newman (2009), Constraints on continued episodic inflation at Long Valley Caldera, based on seismic and geodetic observations, *J. Geophys. Res.*, *114*, B06403, doi:10.1029/2008JB006240.

Fialko, Y., Y. Khazan, and M. Simons (2001), Deformation due to a pressurized horizontal circular crack in an elastic half-space, with applications to volcano geodesy, *Geophys. J. Int.*, *146*(1), 181–190, doi:10.1046/j.1365-246X.2001.00452.x.

Friedrich, W., B. Kromer, M. Friedrich, J. Heinemeier, T. Pfeiffer, and S. Talamo (2006), Santorini eruption radiocarbon dated to 1627–1600 BC, *Science*, *312*(5773), 548, doi:10.1126/science.1125087.

Hardy, D. A., and A. C. Renfrew (Eds.) (1990), *Thera and the Aegean World III: Chronology, Proceedings of the Third Congress*, Thera Found., London.

Harris, R., and P. Segall (1987), Detection of a locked zone at depth on the Parkfield, California, segment of the San Andreas fault, *J. Geophys. Res.*, *92*(B8), 7945–7962, doi:10.1029/JB092iB08p07945.

Heiken, G., and F. McCoy (1984), Caldera development during the Minoan eruption, Thira, Cyclades, Greece, *J. Geophys. Res.*, *89*(B10), 8441–8462, doi:10.1029/JB089iB10p08441.

Manning, S., C. Ramsey, W. Kutschera, T. Higham, B. Kromer, P. Steier, and E. Wild (2006), Chronology for the Aegean Late Bronze Age 1700–1400 BC, *Science*, *312*(5773), 565–569, doi:10.1126/science.1125682.

McTigue, D. (1987), Elastic stress and deformation near a finite spherical magma body: Resolution of the point-source paradox, *J. Geophys. Res.*, *92*(B12), 12,931–12,940, doi:10.1029/JB092iB12p12931.

Mogi, K. (1958), Relations between the eruptions of various volcanoes and the deformations of the ground surfaces around them, *Bull. Earthquake Res. Inst. Univ. Tokyo*, *36*, 99–134.

Newman, A. V., T. H. Dixon, and N. Gourmelen (2006), A four-dimensional viscoelastic model for deformation of the Long Valley Caldera, California, between 1995 and 2000, *J. Volcanol. Geotherm. Res.*, *150*(1–3), 244–269, doi:10.1016/j.jvolgeores.2005.07.017.

Okada, Y. (1985), Surface deformation due to shear and tensile faults in a half-space, *Bull. Seismol. Soc. Am.*, *75*, 1135–1154.

Phillips, E. H. (2004), Collapse and resurgence of the Valles caldera, Jemez Mountains, New Mexico: $^{40}Ar/^{39}Ar$ age constraints on the timing and duration of resurgence and ages of megabreccia blocks, MS thesis, N. M. Inst. of Min. and Technol., Socorro.

Pyle, D. M., and J. R. Elliott (2006), Quantitative morphology, recent evolution, and future activity of the Kameni Islands volcano, Santorini, Greece, *Geosphere*, *2*(5), 253–268, doi:10.1130/GES00028.1.

Sigmundsson, F., et al. (2010), Intrusion triggering of the 2010 Eyjafjallajökull explosive eruption, *Nature*, *468*(7322), 426–430, doi:10.1038/nature09558.

Sigurdsson, H., et al. (2006), Marine investigations of Greece's Santorini Volcanic Field, *Eos Trans. AGU*, *87*(34), 337, doi:10.1029/2006EO340001.

Stiros, S. C., P. Psimoulis, G. Vougioukalakis, and M. Fyticas (2010), Geodetic evidence and modeling of a slow, small-scale inflation episode in the Thera (Santorini) volcano caldera, Aegean Sea, *Tectonophysics*, *494*, 180–190, doi:10.1016/j.tecto.2010.09.015.

Yang, X., P. M. Davis, and J. H. Dieterich (1988), Deformation from inflation of a dipping finite prolate spheroid in an elastic half-space as a model for volcanic stressing, *J. Geophys. Res.*, *93*(B5), 4249–4257, doi:10.1029/JB093iB05p04249.

L. Feng, Earth Observatory of Singapore, Nanyang Technological University, 50 Nanyang Ave., Block N2-01a-15, Singapore 639798.

Y. Jiang, Rosenstiel School of Marine and Atmospheric Sciences, University of Miami, 4600 Rickenbacker Cswy., Miami, FL 33149, USA.

E. Karagianni, D. Panagiotopoulos, C. Papazachos, and D. Vamvakaris, Geophysical Laboratory, Aristotle University of Thessaloniki, PO Box 352-1, GR-54006 Thessaloniki, Greece.

F. Moschas, V. Saltogianni, and S. Stiros, Department of Civil Engineering, University of Patras, GR-26500 Patras, Greece.

A. V. Newman, School of Earth and Atmospheric Sciences, Georgia institute of Technology, 311 Ferst Dr., Atlanta, GA 30332, USA. (anewman@gatech.edu)

P. Psimoulis, Institute of Geodesy and Photogrammetry, Schafmattstrasse 34, CH-8093 Zurich, Switzerland.